Soft Matter

# ARGET-ATRP Synthesis and Swelling Response of Compositionally Varied Poly(methacrylic acid-co-N, N-diethylaminoethyl methacrylate) Polyampholyte Brushes



| | |
|---|---|
| Journal: | *Soft Matter* |
| Manuscript ID | SM-ART-04-2018-000882.R1 |
| Article Type: | Paper |
| Date Submitted by the Author: | 21-Jun-2018 |
| Complete List of Authors: | Ramirez, Rachel; University of Tennessee, Chemistry<br>Woodcock, Jeremiah; National Institute of Standards and Technology, Material Measurement Laboratory<br>Kilbey, S.; University of Tennessee, Chemistry |
| | |



# ARGET-ATRP Synthesis and Swelling Response of Compositionally Varied Poly(methacrylic acid-*co*-N, N-diethylaminoethyl methacrylate) Polyampholyte Brushes

*Rachel Ramirez*[a], *Jerimiah Woodcock*[a] *and S. Michael Kilbey II*[a,b]*

[a]Department of Chemistry, University of Tennessee Knoxville, Tennessee 37996, United States

[b]Department of Chemical and Biomedical Engineering, University of Tennessee Knoxville, Tennessee 37996, United States

* Email: mkilbey@utk.edu

## Abstract

Modifying the composition of polyampholytes, which are comprised of charge-positive and charge-negative repeat units, directly contributes to trade-offs between charge and structure, which are externally regulated by solution pH and added salt. Here, the relative ratio of anionic and cationic comonomers is varied to tailor the stimuli-responsiveness of poly(methacrylic acid-*co*-*N*,*N*-diethylaminoethyl methacrylate) (P(MAA-*co*-DEAEMA)) brushes to changes in solution pH and an added zwitterion. These systems display a strong dependence on excess repeating units of either type and the random incorporation appears to facilitate self-neutralization of charges. Pseudo-living growth with smooth comonomer incorporation is achieved using activators regenerated by electron transfer atom transfer radical polymerization (ARGET ATRP), creating well-defined brushes. *In situ* ellipsometry measurements of solvated brush thickness indicate that at low and high pH, the brushes display polyelectrolyte behavior with a strong compositional dependence, but at intermediate pH values, the brushes show the characteristic collapse attributed to self-neutralization of polyampholytes. The polyampholyte brushes maintain these patterns of behavior across all compositions and in the presence of an added zwitterion, which contributes additional hydrophobic character as evidenced by decreases in the swollen layer thicknesses. The response of the P(MAA-*co*-DEAEMA) brushes to the organic osmolyte

betaine is consistent with its tendency to stabilize proteins and peptides in a chaotropic fashion. These studies add perspective to efforts to manipulate sequence in polyampholytic polymers, support broader efforts to tailor interfacial soft films for applications in biotechnology and sensing, and understand aggregation and stability of biological polymers.

## Introduction

Polymer brushes are assemblies of end-tethered chains that are anchored by one end to a surface or interface at densities high enough that adjacent chains overlap laterally. This crowding causes chains to adopt a stretched conformation in order to reduce repulsive inter-chain interactions. Polyelectrolyte brushes are an important class of polymer brushes containing ionizable groups along the polymer chain, and they have been extensively studied due to their application in colloidal stabilization,[1] lubrication,[2,3] and surface protection,[4] as well as in biotechnology[5] and the development of "smart" interfacial layers that respond to one or more stimuli[6] or have utility as biomedical constructs.[5] Polyelectrolyte brush systems have been extensively examined by theory,[7–11] simulation,[12–15] and experiments,[16–21] and from these studies it is appreciated that the dissociation of charged groups and influx of counterions into the brush in order to compensate charge causes intra- and inter-chain repulsion that modulates swelling. This inter-relationship between conformation and charge, which is affected by pH and the type and concentration of salts or other electrolytes, not only leads to complex behaviors but also engenders their use in myriad applications.

Additional complexity in polyelectrolyte phase behavior can be created by incorporating both cationic and anionic groups along the same polymer chain, creating what are termed polyampholytes. Polyampholytes are made from pairs of monomers that are weak acids and weak bases,[22–25] strong acids and strong bases,[26] or a combination of strong and weak electrolytic groups. [27–30] In the case of polyampholytes consisting of repeating units that are weak electrolytes, the overall response can be altered by varying the copolymer composition during

synthesis and by changing the degree-of-dissociation of the repeat units by using solution pH or ionic strength to manipulate the equilibrium between charged and uncharged states.[31,32] The ability to alter the number of positively- and negatively-charged groups on a polyampholyte gives rise to the situation where the net charge on the chain is zero, which is known as the isoelectric point.[33] At and around the isoelectric point, pairing between the oppositely charged groups in the same or neighboring chains leads to a collapse. At high charge asymmetry, either far above or below the isoelectric point, polyampholytes will behave like a polyanion or a polycation polyelectrolyte due to an excess of charge-negative or charge-positive groups, respectively.[23,34]

Sequence matters in polymer systems, and this is also true in both synthetic and natural polyampholytes.[35–38] In the area of polyampholyte brushes, most of the focus to-date has been on multiblock[7,22,24,25,27,32,34] or strictly alternating arrangements of comonomers.[39–41] For example, through molecular dynamics simulations, Cao et al.[39] and Baratlo et al.[40,41] examined how alternating arrangements of charge-positive and charge-negative comonomers affect the structure of polyampholyte brushes, specifically varying the number of cationic and anionic repeat units arranged in alternating fashion from one to a few monomers in length. They showed that for flexible polyampholytes (PAs) having longer "runs" of comonomers arranged in an alternating sequence, electrostatic interactions between oppositely charged sequences near either planar or spherical surfaces tend to collapse the chains. In these alternating designs, there also is a strong dependence on the interplay between chain stiffness and electrostatics that promotes buckling of chains in order to compensate charge when the "run length" of similarly charged repeat units increases.[39–41] These factors lead to complex dependencies of chain conformation and brush structure on stiffness, added salt, and grafting density.

The responsive behavior and conformational properties of weak polyampholyte diblock copolymer brushes have been theoretically and experimentally studied by Genzer et al.[25] and by

Linse and coworkers.[7] Genzer and co-workers synthesized poly((dimethyl aminoethyl methacrylate)-*block*-poly(acrylic acid)) (DMAEMA-*b*-PAA) brushes and used ellipsometry to study their swelling response to changes in pH. Trends in ellipsometric angles Ψ and Δ were used to interpret the total thickness of the wet brush and to produce a description of the structural changes. At high and low pH, the brushes were swollen while at the intermediate pH values, they observed an increase in Δ (or Ψ), which indicates a decrease in the thickness of the brush. They reasoned that the collapse was due to pairing of charge-positive and charge-negative repeat units either within a chain (self-collapsing) or between neighboring chains.[25] This behavior is consistent with earlier results by Linse and co-workers, who used mean-field lattice theory to study the structure of diblock polyampholyte brushes grafted on a planar substrate (as well as on a spherical substrate).[7] They showed that chain conformation depended on the relative charge of the blocks, which is controlled by solution pH. When the polyampholyte brush is at a fairly low charge ratio, two types of chain conformations exist simultaneously: blocks are either stretched or coiled (collapsed). At a relatively high charge ratio they found that a hairpin bend at the junction between the two blocks exists, driven by electrostatic interactions between the oppositely charged blocks.[7] This allows the diblock chains to self-neutralize charge, which collapses the layer due to the hydrophobic effect. This characteristic pattering of swelling behavior of polyampholyte multiblock brushes was also observed by Brittain and coworkers,[22,27] who used a surface initiated atom transfer radical polymerization (SI-ATRP) (typically referred to as a ‘‘grafting from’’ approach) to synthesize poly(acrylic acid-*b*-2-vinyl pyridine) and poly(acrylic acid-*b*-4-vinyl pyridine) diblock copolymer brushes. Layer thicknesses determined by ellipsometry showed that the chains of the polyampholyte brush were stretched at low and high pH values but collapsed at intermediate pH values. Yu et al. used AFM measurements to deduce that the collapses of polyampholytic chains around the isoelectric point causes a roughening of the surface.[24]

Beyond these examples of multiblock polyampholyte brushes, Tran and coworkers examined the behavior of random polyampholyte brushes comprised of a stoichiometric amount of 2-(dimethylamino) ethylmethacrylate (DMAEMA) and methacrylic acid (MAA).[28,29] These polyampholytes were synthesized via surface-initiated ATRP and used to study how variations in the grafting density of chains affected the swelling behavior of the polyampholyte brushes. Neutron reflectometry also was used to determine monomer volume fraction profile as a function of pH. From these measurements, they determined at pH = 2, for the two different grafting densities studied (0.193 and 0.132 chains $nm^{-2}$), the chains are stretched and the polyampholyte brush acts as a charge-positive polyelectrolyte brush. On the other hand, over the pH range of low net charge (near the isoelectric point), the chains are collapsed, with the less-dense brush being significantly more collapsed, likely due to a greater ability for ion pairing between chains.

Within these works, most efforts to synthesize polyampholyte brushes utilize surface-initiated ATRP with sacrificial initiator added to achieve control, which also enables free chains to be recovered, characterized and used as proxies to describe the surface-tethered chains of the brush. Though standard ATRP is well known for its ability to synthesize well-defined polymers and copolymers of specific composition and low polydispersity,[42–44] the variant known as ARGET-ATRP presents certain advantages for controlled polymerization.

Activators regenerated by electron transfer (ARGET) ARTP is a derivative form of ATRP in which reducing agents, such as ascorbic acid or tin(II) 2-ethylhexanoate is used to generate the oxygen-sensitive Cu(I) catalyst species *in situ* from a higher oxidation state Cu(II) species. Cu(I) activates the polymerization while Cu(II) reversibly deactivates growing polymer chains and through these reactions, an equilibrium that favors “dormant” chains and minimizes irreversible termination reactions is established.[45–47] The use of a reducing agent allows for less stringent conditions to initiate the polymerization, improves tolerance to oxygen, and in comparison to traditional ATRP, ARGET ATRP uses significantly lower concentrations of copper catalyst (down

to ppm levels). ARGET ATRP also offers the advantage (compared to traditional ATRP) of significantly reducing side reactions of the metal/ligand catalyst complex. This feature allows ARGET ATRP to reach higher levels of monomer conversion and improve crossover by retaining chain end functionality, thereby enabling copolymers of higher molecular weight to be prepared.[48–50] As the concentration of the copper catalyst is lower, the likelihood of side reactions and termination events is reduced, which enhances control over the polymerization.[45,46,51,52] Together, these features make ARGET ATRP an attractive method for preparing polyampholyte brushes, especially brushes grown from surfaces where there is a low number of active chain ends due to surface densities of chains that are typically of the order of $10^{15}$ or $10^{16}$ ch $m^{-2}$ (chains per $m^2$). ARGET ATRP also provides control in polymerizations involving amine-containing monomers, which has advantages in copolymerizations, allowing for control over the polymers overall compositions and smooth incorporation of comonomers.[53–55]

With these as motivation, we demonstrate the utility of ARGET ATRP for the synthesis of poly(methacrylic acid-*co*-diethylaminoethyl methacrylate) P(MAA-*co*-DEAEMA) across a range of copolymer compositions with excellent control, as evidenced through kinetic studies. This approach is then translated to produce the corresponding polyampholytic brushes having different ratios of charge-positive and charge-negative weak electrolytic repeat units. ARGET ATRP was chosen for its tolerance to amine containing monomers, and charge-negative MAA repeating units were obtained by hydrolysis of the *tert*-butyl ester of *tert*-butyl methacrylate. Finally, a series of swelling studies were performed to examine how copolymer composition affects structural response of random polyampholyte brushes of various composition as pH is changed and betaine a zwitterion is added.

## Experimental Section

### Materials

*tert*-Butyl methacrylate (tBMA, 98%, Aldrich) and *N*,*N*-Diethylaminoethyl methacrylate (DEAEMA, 99%, Aldrich) were passed through a basic alumina column to remove inhibitor. Dry anisole (Aldrich, 99%) was obtained by distillation after stirring over $CaH_2$ overnight. All other chemicals, including copper (II) bromide, ethyl 2-bromoisobutyrate (EBIB, 97%), *tris* (2-pyridylmethyl) amine (TPMA, 98%), tin (II) ethylhexanoate (Sn(II)Oct, 98%), anhydrous tetrahydrofuran (THF, 99%), and Betaine (98%)) were purchased from Aldrich and used as received.

### General characterization methods

Number-average molecular weights, $M_n$, and dispersities of poly(*tert*-butyl methacrylate-*co*-diethylaminoethyl methacrylate) P(*t*BMA-*co*-DEAEMA) copolymers were determined by gel permeation chromatography (GPC) on a Tosoh EcoSEC GPC fitted with two Tosoh TSKgel SuperMultiporeHZ-M columns 4μ (4.6 x 150 mm) and a TSKgel SuperMultiporeHZ-M guard column. Measurements were made at 40 °C using tetrahydrofuran (THF) with 5% triethyl amine as the mobile phase at a flowrate of 1 mL/min. The EcoSEC Data Analysis package (version 1.04) and conventional calibrations using polystyrene (PS) standards of narrow dispersity (Polymer Laboratories, Inc.) were used to analyze macromolecular characteristics of the P(*t*BMA-*co*-DEAEMA) copolymers. $^1$H NMR spectra were acquired using a Varian Mercury 300 MHz NMR spectrometer. When the kinetics of ARGET ATRP were being followed, aliquots of the polymerization solution were taken at regular time intervals using a nitrogen-purged syringe and analyzed immediately by $^1$H NMR spectroscopy to determine conversion. Polymer film thicknesses were measured using a Beaglehole Instruments phase-modulated Picometer ellipsometer, which uses a 632.8 nm HeNe laser as the incident light source. Ellipsometric

angles were measured at multiple angles ranging from 60° to 80° in 1° increments. The angle-dependent ellipsometric data were fit using a "slab-like" model to determine layer thicknesses of the dry brushes in air as well as in aqueous buffer solutions. Goodness-of-fit expressed as chi-square, $\chi^2$, which is characteristic of the accuracy of the fit and spread of the data, was better than $10^{-3}$ for dry brushes and ~$10^{-2}$ or better for solvated brushes. Data and model fits are presented in the ESI†. Dry layer thicknesses are reported as the average of multiple measurements acquired from at least 3 replicate samples. Measurements were made in a series of 30 mM buffers having pH = 3, 4, 5, 6, 7, 8 and 9 (± 0.1) and an ionic strength of 30 mM. Recipes for the buffer solutions can be found in the ESI†.

**Synthesis of poly(*tert*-butyl methacrylate-*co*-diethylaminoethyl methacrylate) (P(*t*BMA-*co*-DEAEMA)) via ARGET ATRP**

All copolymer syntheses were run using a total monomer to initiator ratio, [M]:[I] = 1000:1, while keeping both the total amount of monomer constant at 2.5 M and the copper(II) concentration at 100 ppm. As a representative example, a synthesis is detailed for a copolymer targeted to be 20% DEAEMA (nominally) on a molar basis. $CuBr_2$ (1.01 mg, 0.0045 mmol) and TPMA (5.20 mg, 0.018 mmol) were added to a dry, 50 mL three-neck round bottom flask. The flask was sealed with rubber septa and purged with dry nitrogen. Then, anisole (2 mL) was added using a nitrogen-purged syringe. This solution was maintained at room temperature for 30 minutes to allow the catalyst complex to form. Once the complex had formed, as indicated by the solution turning a bright yellow color, more anisole (6 mL) was added to the flask via a nitrogen-purged syringe. A previously prepared solution of *tert*-butyl methacrylate (5.70 mL, 35.2 mmol), DEAEMA (1.80 mL, 8.80 mmol) and EBIB (8.50 mg, 0.044mmol) in 1 mL of dry anisole was then added slowly to the flask via a nitrogen-purged syringe. Finally, tin (II) ethylhexanoate (20.1 mg, 0.05 mmol), which had been dissolved in dry anisole (1mL), was added immediately to the flask. Once the tin (II) ethylhexanoate was added, four freeze-pump-thaw cycles were used

to remove any dissolved $O_2$. After the final thawing of the contents of the flask, it was then lowered into an oil bath thermostatted at 35 °C to start the polymerization. The kinetics of polymerization were monitored by taking aliquots every 60 min. The polymerization was quenched after 480 min by submerging the flask into liquid nitrogen. After thawing, the polymer was purified by precipitation into approximately 100 mL of an 80/20 (v/v) mixture of hexanes and ethyl ether that was maintained at −78 $^{o}$C using a dry ice/acetone bath and isolated by gravity filtration. After drying in vacuum, the recovered P(*t*BMA-*co*-DEAEMA) copolymer was analyzed by GPC and $^{1}$H NMR spectroscopy. Conversions based on $^{1}$H NMR were 66% ± 2%.

**Synthesis of 3-(2-Bromoisobutyramido)propyl(trimethoxy)silane**

Preparation of an initiator that could be tethered to inorganic surfaces followed protocols described by Tugulu et al.[56] Rigorously dried glassware and an inert argon atmosphere were used and all transfers were done using dried, argon-purged syringes. A solution consisting of 3-aminopropyltrimethoxysilane (0.18 mL, 0.8 mmol) and triethylamine (0.12 mL, 0.8 mmol) in 10 mL of anhydrous THF was prepared in a 50 mL round bottom flask. Then, 2-bromoisobutyryl bromide (0.1 mL, 0.8 mmol) was added dropwise. The solution was then placed in an ice bath and stirred for 3 h; it was then removed from the ice bath and stirred for another 10 h at room temperature. To purify the product, triethylammonium bromide was removed by gravity filtration and the solvent was slowly removed from the filtrate by evaporation under reduced pressure. The product, 3-(2-bromoisobutyramido)propyl(trimethoxy)silane, was analyzed by $^{1}$H NMR spectroscopy (300 MHz): $\delta$ 6.87 (s, 1H), 3.53 (s,9H), 3.22 (m, 2H), 1.91 (s, 6H), 1.62 (m, 2H), 0.62 (t, $J$= 8.12 Hz, 2H). These are consistent with results from Tugulu et al.[56]

**Immobilization of the ARGET ATRP silane initiator onto silicon surfaces**

Silicon wafers (1 × 1.2 cm; Silicon Quest) were cleaned by immersion in a “piranha acid” solution [7:3 ($H_2SO_4$/$H_2O_2$)] for 45 min at 100 $^{o}$C. (*Caution*: Piranha acid is a strong acid and

strong oxidizer.) The surfaces were removed, rinsed with copious amounts of water, and dried under a nitrogen stream. The surfaces were then irradiated via ozonolysis for another 45 min using a NovaScan PSD Series ozone generator to ensure complete oxidation of groups on the surface. The cleaned wafers were then immersed for 6 h in a 40 mM solution of 3-(2-bromoisobutyramido)propyl(trimethoxy)silane in anhydrous THF. After allowing for self-assembly the initiator-functionalized wafers were rinsed with anhydrous THF, dried with a stream of nitrogen, and then transferred to the Schlenk tube used for growing brushes by surface initiated ARGET ATRP. The surface functionalization procedure consistently yielded initiator layers having a thickness of 2-3 nm, as measured by multi-angle ellipsometry.

**Synthesis of polymer brushes via surface initiated ARGET ATRP**

As an example, the synthesis of a copolymer brush containing 20% DEAEMA (nominal composition) on a molar basis is described. A home-built perforated glass platform was inserted into a Schlenk tube equipped with a magnetic stir bar. The platform holds several initiator-decorated silicon substrates level above the stirrer, which allows replicate samples to be produced during a single polymerization. The initiator-functionalized wafers were placed face-up on the platform and the Schlenk tube was purged with nitrogen to ensure the contents were in an inert atmosphere. The remainder of the synthesis was completed with the contents under a positive pressure of nitrogen. $CuBr_2$ (1.05 mg, 0.0045 mmol), TPMA (5.20 mg, 0.018 mmol) and dry anisole (2 mL) were added to the Schlenk tube via syringe and the solution was then stirred for 30 minutes. A solution containing the comonomers in the appropriate ratio was prepared separately in a clean, dry vial the appropriate molar ratio – for this example, *t*BMA (5.70 mL, 35.2 mmol), and DEAEMA (1.80 mL, 8.80 mmol) were mixed. Next, the sacrificial initiator, EBIB, (8.85 mg, 0.044 mmol) was added along with dry anisole (2 mL). This solution of comonomers and sacrificial initiator was then added to the Schlenk tube via a nitrogen-purged syringe. In all cases, the comonomer solution covered the initiator-decorated wafer. Finally, a

separately-prepared solution of tin (II) ethylhexanoate (20 mg, 0.05 mmol) dissolved in anisole (1 mL) was added to the tube via a nitrogen- purged syringe. The Schlenk tube then was immediately sealed and lowered into liquid nitrogen to begin a sequence of four freeze-pump-thaw cycles. After the final thaw, the Schlenk tube was lowered into an oil bath set at 35 $^{o}$C to initiate the polymerization. The mixture was stirred at 500 rpm. After 600 min, the polymerization was quenched by opening the Schlenk tube to the atmosphere and freezing the contents in $LN_2$. After thawing, the surfaces were removed and cleaned by rinsing with dichloromethane (Fisher, reagent grade) followed by sonication for 10 min in dichloromethane to ensure that any physisorbed polymer generated from sacrificial initiator (EBIB) present in solution was removed. The dry film thicknesses of P(*t*BMA-*co*-DEAEMA) brushes were determined via ellipsometry. Free polymer present in the solution was recovered by precipitation into approximately 100 mL of an 80/20 (v/v) mixture of hexanes and ethyl ether that was maintained at −78 $^{o}$C using a dry ice/acetone bath. Following isolation, purification, and drying, these "free" polymer chains were analyzed via GPC and $^{1}$H NMR spectroscopy.

**Generation of P(MAA-*co*-DEAEMA) brushes via post-polymerization modification**

The tert-butyl groups of *t*BMA repeat units were cleaved to yield the polyampholyte, P(MAA-*co*-DEAEMA), by immersing P(*t*BMA-*co*-DEAEMA) brush-modified wafers in a solution (~3.7 mL) of dichloromethane containing 30% trifluoroacetic acid (TFA) for 30 minutes.[57] The wafers were removed from the TFA solution, rinsed with copious amounts of THF and then water. Finally, they were dried using a stream of dry nitrogen gas. The thicknesses of the deprotected brushes were measured at a few different locations on each surface by multi-angle ellipsometry

**Ellipsometric swelling studies of P(MAA-*co*-DEAEMA) brushes**

Brush-modified wafers were secured to a custom-built Teflon holder that fits in a cylindrical glass cell used for swelling or adsorption measurements.[58–61] Buffer solutions at pH = 9, 8, 7, 6, 5, 4 and 3 (each ± 0.1 pH unit) were prepared at an ionic strength of 3 mM and introduced to the glass cell individually. To mitigate cross-contamination when changing pH, after measurements in a given buffer solution, the electrolyte solution was withdrawn and the cell was flushed with copious amounts of deionized water (refilling and draining). The wafer and cell were flushed three times using deionized water before a new buffer solution was introduced into the cell. The polymer brushes were allowed to equilibrate in the buffer solution for 20 min before multi-angle ellipsometry measurements were made. While the brush was equilibrating, the brush-modified surface was re-aligned in the filled cell to ensure fluid changes did not alter the measurement geometry.

## Results and Discussion

### Kinetic studies of solution synthesis P(*t*BMA-*co*-DEAEMA) copolymers

While ATRP is tolerant to many functional groups, in practice, acrylic acid and methacrylic acid require additional considerations because these charge-negative monomers interact or react with the basic metal/halide complexes. Side reactions, such as formation of metal carboxylates, result in inefficient deactivators that lead to loss of control. Furthermore, the metal carboxylates cannot be reduced to reactivate chain growth in ATRP.[62] A standard approach, therefore, is to conduct the ATRP using the "protected" monomers *tert*-butyl acrylate (*t*BA) or *tert*-butyl methacrylate (*t*BMA), followed by hydrolysis or pyrolysis of the *tert*-butyl ester "protecting" groups to produce the corresponding weak polyacid, either poly(acrylic acid) or poly(methacrylic acid).[22,27,63] Also, it is known that tertiary amines are capable of reducing the higher oxidation state metal/ligand catalyst complex to the active form, resulting in an increase

in polymerization and potential loss of control.[55] Therefore, ARGET ATRP was used in order to reduce the possibility of side reactions and termination events, and ensure control over chain growth. Furthermore, because polymerizations intitated from flat surfaces are difficult in part because of there being a low number of active chains (usually ~$10^{15}$ – $10^{16}$ chains $m^{-2}$), kinetic studies of solution copolymerization were performed in order to elucidate conditions that were pseudo-living/controled, as evidenced by the polymerization adhereing to first order kinetics with a persistant radical population. To this end, P(*t*BMA-*co*-DEAEMA) copolymers were synthesized in anisole at 35 °C via ARGET ATRP using EBIB initiator with a total monomer concentration of 2.5 M. Random copolymers were produced across a wide range of comonomer feed ratios, as seen in Table 1.

**Table 1. Characteristics of P(*t*BMA-*co*-DEAEMA) copolymers.**

| Molar Compositional Ratio tBMA:DEAEMA | Actual Copolymer Composition[a] | $M_n$ (kDa)[b] | Đ[b] |
|---|---|---|---|
| 80:20 | 79:21 | 45.4 | 1.14 |
| 70:30 | 72:28 | 45.8 | 1.12 |
| 60:40 | 61:39 | 48.1 | 1.16 |
| 50:50 | 51:49 | 48.3 | 1.15 |
| 40:60 | 39:61 | 46.3 | 1.16 |
| 30:70 | 28:72 | 45.6 | 1.17 |
| 20:80 | 19:81 | 47.7 | 1.14 |

[a] Determined via $^1$H NMR spectroscopy. [b]Relative to polystyrene standards.

Seven copolymerizations were performed in parallel, varying the [tBMA]/[DEAEMA] comonomer feed ratio to examine the efficacy of ARGET ATRP over a wide range of comonomer compositions. Aliquots were taken every hour throughout the polymerizations and the random copolymers recovered after 8 h of polymerization time were analyzed by $^1$H NMR spectroscopy and GPC. Kinetic plots based on first-order kinetics using monomer conversion determined from $^1$H NMR spectroscopy are shown in Figure 1 for copolymers that were synthesized by ARGET ATRP using comonomer feed ratios of 80/20, 50/50, and 20/80 *t*BMA/DEAEMA. The corresponding figuress for all other compositions can be found in the ESI†. The relationship reflected in each of the plots (including those presented in the ESI†) indicates that the polymerization is first order with respect to monomer conversion for all comonomer compositions. The slope extracted from the kinetic profile of each of the three copolymerizations yields information about the effective rate of the ARGET ATRP reaction, $k_{eff}$: The slope deduced from the kinetic plot for the 80/20 tBMA/DEAEMA copolymerization is 0.0013 $s^{-1}$, which is similar to but smaller than the slopes determined from polymerizations at comonomer ratios of 50/50 and 20/80, which have $k_{eff}$ = 0.0017 $s^{-1}$ and $k_{eff}$ = 0.0018 $s^{-1}$, respectively. These values suggest that increasing the relative abundance of DEAEMA increases the rate of polymerization, which is consistent with the acceleration of ATRP due to tertiary amines seen by Radosz et al.[55] Nevertheless, excellent control is maintained in the ARGET ATRP copolymerization across the range of comonomer feed ratios, which used [monomer]:[EBIB]:[Cu(II)$Br_2$]:[TMPA]:[Sn(II)Oct] = 1000:1:0.1:0.4:1.

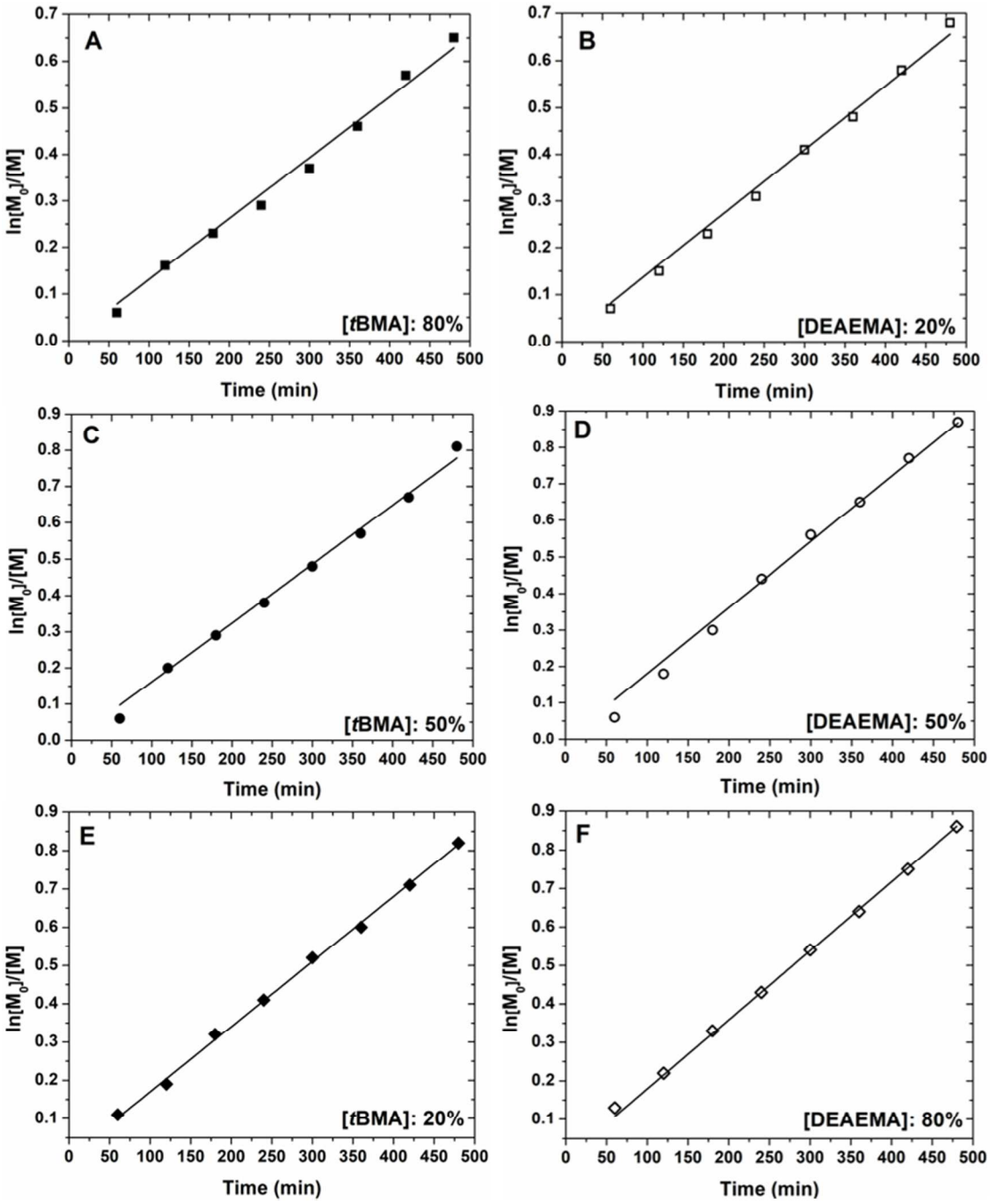


**Figure 1**. Kinetic plots for ARGET ATRP of P(*t*BMA-*co*-DEAEMA) at various comonomer ratios. Plots A and B are for a copolymer targeted to be 80 mol % *t*BMA and 20 mol % DEAEMA; C and D are for the copolymer targeted to be 50 mol % *t*BMA and 50 mol % DEAEMA; and E and F are for the copolymer targeted to be 20 mol % *t*BMA and 80 mol % DEAEMA. All reactions were run in anisole at T=35 °C for 8 h.

This impact of DEAEMA monomer acting as a reducing agent and affecting the rate of polymerization, $R_p$ is expected based on the rate expression developed by Matyjaszewski et al.

$$R_p = k_p K_{eq} [In] \frac{[Cu(I)]}{[Cu(II)X]} [M] \quad (1)$$

In this expression, $k_p$ is the polymerization constant, $K_{eq}$ is the equilibrium constant for propagation, and [M] is the monomer concentration. Assuming steady-state kinetics, as the concentration of the activator, the Cu-metal/ligand complex Cu(I)/L, increases due to reduction of the deactivator, Cu(II)X/L, either by the Sn(II)Oct or the DEAEMA acting as reductant, the rate of polymerization increases.

Although DEAEMA exerts a slight influence on the rate of polymerization, the polymerizations are well controlled. In addition and as shown in Table 1, the overall composition of the polymer closely follows the comonomer feed ratio. Copolymer composition determined by $^1$H NMR spectroscopy agrees with the feed ratio within ± 2 %. This suggests a lack of preference for incorporation of the two methacrylate-based comonomers. Finally, ARGET ATRP resulted in low dispersities that range from 1.12-1.17, which is lower than 50:50 random polyampholyte brushes synthesized by ATRP, which had a dispersity of 1.4.[29] These show that ARGET ATRP provides excellent control over copolymerization of amine containing copolymers across the entire range of comonomer feed ratios.

**Synthesis of P(MAA-*co*-DEAEMA) Polymer Brushes**

With useful conditions for ARGET ATRP resolved through kinetic studies of solution polymerizations, P(MAA-*co*-DEAEMA) brushes on flat silicon substrates were created via the "grafting from" approach illustrated in Scheme 1. As noted previously, the protected form of MAA was used, and *t*-butyl groups were subsequently removed by acid-catalyzed hydrolysis.

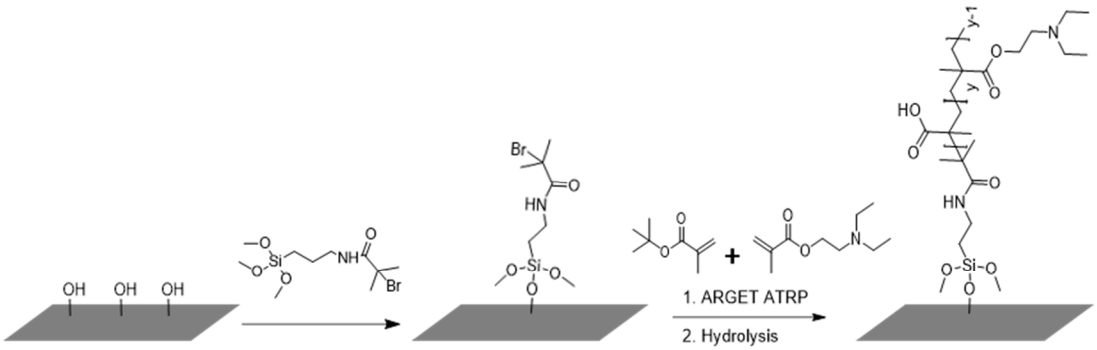


**Scheme 1**. Synthesis of P(MAA-*co*-DEAEMA) on silicon substrates using ARGET ATRP.

In these polymerizations, free EBIB initiator was added to the solution to set a monomer-to-initiator ratio of 1000. It is well-accepted that free initiator is required to achieve controlled growth chains of surface-attached chains.[64–66] P(MAA-*co*-DEAEMA) brushes were synthesized across comonomer feed ratios ranging from 80 mol % to 20 mol % DEAEMA and the recovered free chains used as proxies for the surface-tethered chains. Characterization by GPC shows that the free copolymer chains have narrow dispersities ($Đ < 1.2$), and these are shown in Table 2 along with $M_n$ values (relative to PS standards) and compositional information obtained by $^1$H NMR spectroscopy. The dispersities and molecular weights are similar to those obtained from kinetic studies and analysis by $^1$H NMR spectroscopy again shows that comonomer incorporation is smooth and follows the comonomer feed ratio. Furthermore, the ellipsometric thicknesses of the deprotected polyampholyte brushes, $H_{PA}$, are large and generally correlate with the number-average molecular weight, which together suggest that the surface is uniformly covered with a dense polymer brush. This contention is supported by AFM images showing homogenous coverage and low values of root mean square roughnesses. (See ESI†.)

**Table 2. Characterization Data for P(MAA-*co*-DEAEMA) and Dry Film Thicknesses**

| *t*BMA:DEAEMA | Mol % DEAEMA[a] | $M_n$ (kDa)[a] | Đ[a] | $H_{elli}$ (nm)[b] | $H_{PA}$ (nm)[c] | σ (Chains/nm$^2$)[d] |
|---|---|---|---|---|---|---|
| 80:20 | 19 | 55.8 | 1.13 | 45±3 | 28±2 | 0.50 |
| 70:30 | 32 | 55.2 | 1.11 | 53±5 | - | 0.59 |
| 60:40 | 42 | 65.1 | 1.15 | 61±4 | - | 0.58 |
| 50:50 | 48 | 68.4 | 1.15 | 78±4 | 59±3 | 0.71 |
| 40:60 | 63 | 44.3 | 1.17 | 63±3 | - | 0.88 |
| 30:70 | 72 | 45.6 | 1.17 | 53±4 | - | 0.72 |
| 20:80 | 83 | 55.3 | 1.12 | 42±3 | 38±3 | 0.50 |

[a] Based on measurement of free chains recovered from solution. [b] Average ellipsometric thickness of "protected" P(tBMA-*co*-DEAEMA) brushes obtained from multiple measurements on replicate samples. [c] Average ellipsometric thickness of deprotected polyampholyte brushes taken from multiple measurements of replicate samples. [d] Based on dry film thickness of P(*t*BMA-*co*-DEAEMA) brushes.

The film thicknesses of the p(*t*BMA-*co*-DEAEMA) brushes, $H_{elli}$, obtained from ellipsometry show an increase in thickness as composition increases up to 50 mol % DEAEMA but then decrease as incorporation of DEAEMA continues to increase. This pattern of behavior seems to not follow molecular weight of the copolymers, which suggests that variations in grafting density across the composition range are impacting thickness, even though each set of surfaces were made using consistent protocols. This general sensitivity of surface-initiated polymerizations, coupled with the fact that grafting density of chains, $\sigma$, is calculated from layer thickness by the dimensional expression $\sigma = H_{elli}\rho N_A/M_n$, provides context as to why the brush characteristics vary substantially across the range of comonomer composition. Another cause for the variations in the grafting density may arise through the use of DEAEMA as a comonomer: it

has been reported that aliphatic tertiary amines can reduce Cu(II) to Cu(I) and produce cation radicals.[55,67,68] Thus, if DEAEMA functioned as an internal reducing agent, it would affect the equilibrium between dormant and active states or lead to additional side reactions and termination events may have a significant impact on the growth of the brush. This would be especially influential in the case of propagation of chains from the surface, where there is a low number density of chains.

There is additional information within the set of data that buttresses the contention that variations are due to the sensitivity of these surface initiated polymerizations: The ratios of brush heights of the parent and deprotected, polyampholyte (PA) brushes, $H_{PA}/H_{elli}$, are compared to the corresponding ratios of molecular weights, $M_{n,PA}/M_n$, and presented in Table 3. As outlined in the ESI†, molecular weights and compositions of the 80/20, 50/50, and 20/80 random copolymers allow the theoretical molecular weight of the polyampholyte brushes to be calculated. In light of the fact that assumptions of constant grafting density, complete transformation of P(tBMA-*co*-DEAEMA) to P(MAA-*co*-DEAEMA) by acid-catalyzed hydrolysis, and constant mass density are invoked, the correspondence between $H_{PA}/H_{elli}$ and $M_{n,PA}/M_n$ as a function of composition is excellent. (See Table 3.) Moreover, the best-fit line describing the relationship between copolymer composition and $H_{PA}/H_{elli}$ extrapolates to 0.54 at $f_{DEAEMA} = 0.0$ and to 0.98 at $f_{DEAEMA} = 1.0$. This self-consistency strongly supports for the notion that variations in brush characteristics are simply inherent to these surface-initiated polymerizations.

**Table 3. Comparison of "Parent" and Polyampholyte Brush Thickness and Molecular Weight Ratios**

| *t*BMA:DEAEMA | Mol % DEAEMA[a] | $M_{n,\,PA}/M_n$ | $H_{PA}/H_{elli}$ |
|---|---|---|---|
| 80:20 | 19 | 0.68 | 0.62 |
| 50:50 | 48 | 0.79 | 0.76 |
| 20:80 | 83 | 0.93 | 0.91 |

[a] Based on measurement of free chains recovered from solution

**Swelling Studies of Polyampholyte Brushes**

The response of P(MAA-*co*-DEAEMA) brushes to changes in pH was investigated by measuring the brush thickness as solution pH was incrementally lowered from pH 9 to 3 at a constant ionic strength of 3 mM. The swelling ratio, $T/T_{dry}$, is used to facilitate comparison of the response of different brushes as a function of pH, as shown in Figure 2, which presents the swelling responses of P(MAA-*co*-DEAEMA) random copolymer brushes synthesized with comonomer compositions of 20, 50, and 80 mol % DEAEMA, respectively.

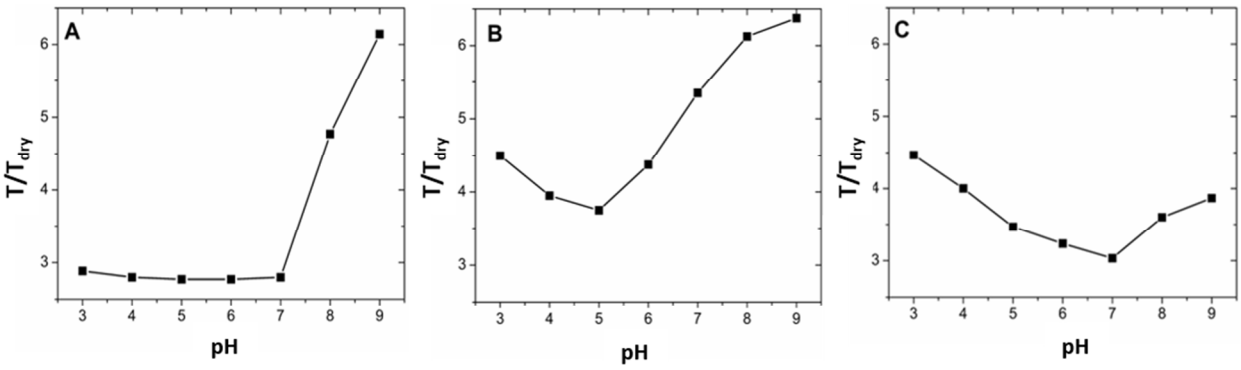


**Figure 2.** Swelling response of p(DEAEMA-*co*-MAA) brushes as a function of pH. Amine content varies, with (A) representing 20 mol % DEAEMA, (B) 50 mol % DEAEMA, and (C) 80 mol % DEAEMA. In each case, the swollen thickness measured by *in situ* ellipsometry is normalized by the thickness of the brush measured in ambient conditions.

The swelling behaviors reflect, in general, polyelectrolyte behavior at low and high pH and polyampholytic character at intermediate pH values. Moreover, they are consistent both with changes in relative amount of the two comonomers and behaviors of confined systems of charged polymers. These aspects are discussed in turn, beginning with the response at low and high pH where the brushes behave like polyelectrolytes.

At low pH values, both the DEAEMA segments and MAA are in their protonated form, rendering DEAEMA repeat units positively charged while MAA repeat units exist in their neutral carboxylic acid form. Previous neutron reflectivity studies by Deodhar et al.[57] show that MAA is strongly hydrophobic when in its neutral (protonated or non-dissociated) form. As a result, the polyampholyte brush containing 20% DEAEMA does not show much swelling due to the dominance of the excess hydrophobic MAA repeat units. At low pH values and as the relative amount of MAA decreases, the DEAEMA exerts greater influence over the swelling behavior: the p(DEAEMA-*co*-MAA) brush that is 50 mol % DEAEMA is more extended than the 20% DEAEMA brush, but less swollen than the 80% DEAEMA brush. In addition, the three swelling curves suggest that the onset at which polybase character manifests at low pH (swelling when DEAEMA is protonated)[69] shifts to higher pH as DEAEMA content increase.

Analogous behavior is observed in the swelling response of the brushes at high pH, where the chains take on poly(acid) character due to deprotonation of MAA repeat units. At a pH = 9, which eclipses the $pK_a$ of homopolymers of DEAEMA ($pK_a$ of the conjugate acid = 7.5) and its monomer ($pK_a$ = 8.8),[70] the 20/80 and 50/50 p(DEAEMA-*co*-MAA) brushes show significant swelling, with T/Tdry ~ 6; the 80/20 p(DEAEMA-*co*-MAA) brush is not as strongly stretched due to the fact that the uncharged DEAEMA repeat units are only slightly hydrophilic.[69,71,72] The behaviors observed at both low and high pH are consistent with the notion that electrolytic group present in abundance exerts greater influence over the swelling behavior.

There are two aspects related to ellipsometric measurements of dry and swollen brushes that merit discussion. First, while the measured swollen thicknesses are normalized by the dry

layer thickness measured for each of the brushes, dry layer thicknesses must be interpreted with caution. As shown by Deodhar et al.,[57] PMAA brushes and copolymer brushes containing MAA and hydroxyethyl methacrylate absorb water from humid environments. Thus, even in the state referred to as "dry", water-soluble brushes may contain a significant fraction of water: Deodhar et al. showed that the volume fraction of water in the dry brush approached 30%, with the apparent trend that higher grafting density led to a lower volume fraction of absorbed water.[57] In the case of these p(DEAEMA-*co*-MAA) brushes, there is no reason to expect that the degree of latent hydration is consistent across the compositions studied. Second and as discussed in our recent studies of polypeptide brushes,[73] because stretching of brush chains in a good solvent produces a smoothly-decaying segment density profile, the "step-like" profile used to fit ellipsometric data underrepresents the height of solvent-swollen brushes, with increasing departure as chain extension increases. For these reasons, the pattern of behavior displayed by a given brush and comparison between the different brushes are more informative than specific values of the swelling ratio.

Another point worth discussing is the apparent change in $pK_a$ exhibited by the p(DEAEMA-*co*-MAA) polyampholyte brushes. As noted by Deodhar et al., the $pK_a$ of PMAA brushes shift to higher values compared to free chains.[57] This change is consistent with behaviors observed by Genzer and coworkers[74] and can be attributed to the local dielectric environment of a brush, which differs from that of solvent water because of the high concentration of repeat units confined near the solid/fluid interface.[74–76] The local dielectric function is affected by the dipole moment of the ion-pairs, the concentration of counterions and co-ions, and the local composition. In addition, because the dielectric function follows the segment density profile of an electrolytic brush,[75,76] the inhomogeneous environment affects the charge dissociation equilibrium due to the varying intermolecular interactions and electrostatic potential.[75] This also has been experimentally observed through titration studies of weak poly(acid) brushes, specifically PAA and PMAA. Ober et al. also showed that the effective $pK_a$ at the film/air interface, $pK_a^{surf}$, is

approximately two units smaller than the $pK_a$ of the bulk material, $pK_a^{bulk}$. This implies that carboxylic acid groups on repeat units further away from the surface are more readily ionized than acid groups near the surface.[77] They suggested that at pH < $pK_a^{surf}$, all of the acid groups are protonated making the poly(acid) brushes relatively hydrophobic and the chains of the brush are collapsed. When the pH approaches $pK_a^{surf}$, the acid groups in the uppermost layer ionize, making the outer region of the brush hydrophilic while a major portion of the chains remain collapsed. They also showed that a small fraction of acid groups located near the solid substrate remain uncharged, even at very high pH. While these behaviors are specific to weak poly(acid)s, it is likely that there are analogous effects in which the local $pK_b$ differs from $pK_b^{bulk}$that occur with a weak poly(base) brush, such as pDEAEMA. Moreover, we would anticipate these effects would add complexity to the pH-mediated swelling behavior of polyampholytic brushes due to the presence of both types of weak electrolytic groups.

Sequence effects will also play a role in how the polyampholyte brushes behave in response to changes in pH. Using Monte-Carlo simulations, Ulrich and coworkers examined how the overall arrangement of repeating units in diblock, alternating, and random copolymer designs influence titration curves of weak polyampholytes.[78] For A-B polyampholytes in which A is a weak acid and B is a weak base, when $pK_a^A$ < pH < $pK_a^B$, both A and B repeating units are fully charged, but when pH < $pK_a^A$ or when pH > $pK_a^B$, only B or A repeats are charged, respectively. With both random and alternating polyampholytes, Ulrich and coworkers saw that titration curves of repeating units of type A (type B) are shifted to smaller (higher) pH values as the ionization of acidic (basic) groups is facilitated, particularly at low salt concentrations where screening is lessened.[78] Their studies show that these effects are more pronounced in an alternating polyampholyte designs compared to random copolyampholytes because the regular, sequential arrangement of charge-positive and charge-negative repeat units facilitates ion-pairing through short-range electrostatic interactions. In addition to ionization of repeat units being

promoted, chain flexibility plays an important role, with flexible polyampholytes adopting more compact conformations upon self-neutralization.[78]

The patterns of behavior displayed in the titration curves of the polyampholyte brushes are consistent with these traits. For all of the p(MAA-*co*-DEAEMA) polyampholytes, when the pH is in an intermediate range, the charge-negative carboxylates of MAA repeat units are neutralized by ion pairing with oppositely charged, quaternized amines of DEAEMA repeating units, leading to a reduction in brush height. Presumably, this is facilitated by the close proximity of charge-negative and charge-positive repeat units, either through short-range interactions within the chain or interactions with neighboring chains in the crowded, confined environment of the brush. In this case, the chains adopt a collapsed conformation and exclude water and counterions from the interfacial layer. This self-neutralization at an intermediate pH, known as the isoelectric point, is associated with classical polyampholyte behavior and has been observed by Brittain and coworkers in their studies of poly(acrylic acid-*b*-2-vinylpyridine) and poly(acrylic acid-*b*-4vinyl pyridine).[27]

In blocky polymer systems, the isoelectric point is sharp and generally well defined; however, in random polymer systems the isoelectric point appears to be less well defined due to the facility with which self-neutralization is achieved through short range interactions along the chain. All of the swelling curves measured for the polyampholytic brushes studied here go through a minimum between $4.5 < pH < 7.5$. In the case of the compositionally symmetric brush (50% DEAEMA; Figure 2b) there is a distinct minimum in swollen thickness at pH = 5, which is assigned as an apparent isoelectric point. Whether conformational entropy prohibits the brush from self-neutralization cannot be inferred from these measurements. Given that the layer does not collapse more strongly, it seems reasonable to posit that some electrolytic groups are neutralized by counterions present in the buffer, which leads to osmotic swelling of the layer.

The swelling behavior of the 50 mol % DEAEMA brush is similar to the behavior observed by Tran and coworkers in their studies of the effect of grafting density on

poly(methacrylic acid-*r*-dimethylaminoethyl methacrylate) random polyampholyte brushes made with a 1:1 comonomer ratio.[29] For a brush having a grafting density of 0.132 ch $nm^{-2}$, they observed a stronger collapse over the range $5 \leq pH \leq 7$ with an isoelectric point between pH = 6.0 and 7.6. Swelling of the layer was evident at pH = 8 and pH = 3 which are characteristic of a polyacid and a polybase brush, respectively. While a symmetric polyampholyte brush having a grafting density of 0.193 ch $nm^{-2}$ remained swollen across the range of pH values studied, in both cases and consistent with the behaviors reported here, the random polyampholyte brushes remain swollen with $T/T_{dry} \approx 3$ when self-neutralized, rather than collapsing toward their dry layer thicknesses.

The behavior of the polyampholyte brushes containing 20 mol% DEAEMA and 80 mol % DEAEMA are also consistent with a tendency for self-neutralization at intermediate pH values, but the presence of excess weak acid and weak base and inherent solubility differences dominate swelling behaviors. (Recall, uncharged MAA is more hydrophobic than uncharged DEAEMA, and charged MAA is more hydrophilic than charged DEAEMA.) The hydrophobicity of uncharged PMAA dominates the behavior of brushes containing 20 mol% DEAEMA, as reflected in the nearly-constant and low values of swelling ratio, $T/T_{dry}$, throughout the window where self-neutralization is observed to occur. The drastic reduction in MAA content in the brush containing 80% DEAEMA allows a comparatively larger, yet modest swelling response, especially across the range of pH values where self-neutralization occurs. In addition, the minimum that may be ascribed to self-neutralization is shifted to higher pH (relative to that of the compositionally symmetric brush). As the percentage of DEAEMA is increased, the location of the minima shifts to higher pH.[79] However, it is unclear whether this shift is a consequence of the onset of poly(base) character coupled with diminished influence of MAA repeat units, or if the relative abundance of DEAEMA repeating units and their quaternization is facilitating ionization of MAA repeating units, causing self-neutralization. Finally, because the local dielectric environment influences the chemical equilibrium between charged and neutral states,[74-

[76] it seems reasonable to conclude that self-neutralization will be similarly affected by the local composition within the polyampholyte brush as well as by the tendency of random polyampholytes to facilitate ionization and self-neutralization.

**Swelling Response in the Presence of Betaine Zwitterion**

The impact of an added zwitterion on the swelling behavior of the polyampholyte brushes was examined by adding the zwitterion, betaine (0.03 M), to the buffer solutions. (This maintains the ionic strength at 30 mM.[80]) The organic osmolyte betaine is classified as non-ionic kosmotrope because it is known to stabilize the folded conformation of proteins by virtue of being excluded from solvation layers.[81] In keeping with this expectation and as seen in Figure 3, the total swelling of the polyampholyte brushes is diminished in the presence of betaine. However, the characteristic shape of the swelling curve of is not altered: At low and high pH, the brushes display polyelectrolyte behavior but at intermediate pH values they exhibit polyampholyte behavior. In addition, the minima that were attributed to self-neutralization of the polyampholyte brushes containing 50 mol % DEAEMA and 80 mol % DEAEMA are also unchanged, while swelling of the polyampholyte brush containing 20 mol % DEAEMA is strongly restricted by the excess MAA repeat units.

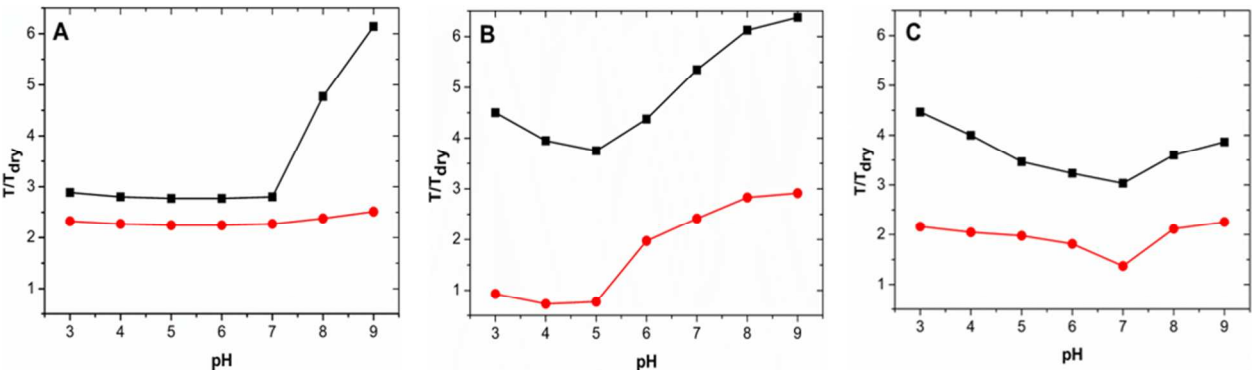


**Figure 3.** Swelling behavior of p(MAA-*co*-DEAEMA) brushes of different composition as a function of pH. The swelling behavior of the original curves (black squares) to the curves obtained from the addition of the zwitterion (red circles) are compared with the amine content in

the polyampholytes increasing from (A) 20 mol % DEAEMA, (B) 50 mol % DEAEMA, and (C) 80 mol % DEAEMA. The lines connecting the points are merely meant to guide the eye.

Given the consistency between the patterns of behaviors observed in buffered solution and in buffers containing the zwitterion, it appears that the main impact of added zwitterion swelling is to effectively render the polyampholyte brushes more hydrophobic. The decrease in swelling exhibited at all pH values may be a result of betaine adding hydrophobicity to the chains by pairing with charged groups along the chain, or it may be caused by exclusion of the small molecule osmolyte from the solvation shell around the polyampholyte chains. This latter speculation is consistent with a growing body of evidence suggesting that depletion forces are the general mechanism by which proteins and peptides are stabilized by non-ionic organic osmolytes like betaine.[81–85]

**Conclusions**

We describe the use of ARGET ATRP to synthesize random copolymers of DEAEMA and *t*BMA, and use conditions identified through solution polymerization to create polyampholyte brushes via "grafting from" method followed by chemical conversion to p(MAA-*co*-DEAEMA) polyampholytes. Although an excess of either comonomer influences the swelling behavior, multiangle ellipsometry measurements show that the random copolyampholyte brushes follow polyelectrolyte behavior at low and high pH, but polyampholytic character marked by a self-neutralization is observed at intermediate pH values. While the extent of swelling is decreased when betaine a zwitterion is added to the solution, the mode of action appears to share commonality with how organic osmolytes stabilize intrinsically disordered proteins and peptides. Thus, the extension of ARGET ARTP to create compositionally-tuned polyampholyte brushes and the use of those brushes as models to understand swelling response in different electrolytic environments may provide a basis to address structural responses and aggregation of biological polymers and the action of cryoprotectants.

**Acknowledgements**

This work was supported by the National Science Foundation (Award Nos. CBET 1133320 and 1512221).

**References**

1 P. Pincus, Colloid stabilization with grafted polyelectrolytes, *Macromolecules*, 1991, **24**, 2912–2919.
2 M. Chen, W. H. Briscoe, S. P. Armes and J. Klein, Lubrication at Physiological Pressures by Polyzwitterionic Brushes, *Science*, 2009, **323**, 1698–1701.
3 J. Klein, Repair or Replacement: A Joint Perspective, *Science*, 2009, **323**, 47–48.
4 A. Wittemann, B. Haupt and M. Ballauff, Adsorption of proteins on spherical polyelectrolyte brushes in aqueous solution, *Phys. Chem. Chem. Phys.*, 2003, **5**, 1671–1677.
5 M. Ballauff and O. Borisov, Polyelectrolyte brushes, *Curr. Opin. Colloid Interface Sci.*, 2006, **11**, 316–323.
6 F. Zhou and W. T. S. Huck, Surface grafted polymer brushes as ideal building blocks for "smart" surfaces, *Phys Chem Chem Phys*, 2006, **8**, 3815–3823.
7 N. P. Shusharina and P. Linse, Oppositely charged polyelectrolytes grafted onto planar surface: Mean-field lattice theory, *Eur. Phys. J. E*, 2001, **6**, 147–155.
8 L. Chen, H. Merlitz, S. He, C.-X. Wu and J.-U. Sommer, Polyelectrolyte Brushes: Debye Approximation and Mean-Field Theory, *Macromolecules*, 2011, **44**, 3109–3116.
9 R. Israels, F. A. M. Leermakers and G. J. Fleer, On the theory of grafted weak polyacids, *Macromolecules*, 1994, **27**, 3087–3093.
10 E. B. Zhulina, T. M. Birshtein and O. V. Borisov, Theory of ionizable polymer brushes, *Macromolecules*, 1995, **28**, 1491–1499.
11 T. Jiang, Z. Li and J. Wu, Structure and Swelling of Grafted Polyelectrolytes: Predictions from a Nonlocal Density Functional Theory, *Macromolecules*, 2007, **40**, 334–343.
12 O. J. Hehmeyer, G. Arya, A. Z. Panagiotopoulos and I. Szleifer, Monte Carlo simulation and molecular theory of tethered polyelectrolytes, *J. Chem. Phys.*, 2007, **126**, 244902–244913.
13 F. S. Csajka and C. Seidel, Strongly Charged Polyelectrolyte Brushes: A Molecular Dynamics Study, *Macromolecules*, 2000, **33**, 2728–2739.
14 C. Seidel, Strongly Stretched Polyelectrolyte Brushes, *Macromolecules*, 2003, **36**, 2536–2543.
15 N. A. Kumar and C. Seidel, Polyelectrolyte Brushes with Added Salt, *Macromolecules*, 2005, **38**, 9341–9350.
16 P. Guenoun, A. Schalchli, D. Sentenac, J. W. Mays and J. J. Benattar, Free-standing black films of polymers: a model of charged brushes in interaction, *Phys. Rev. Lett.*, 1995, **74**, 3628–3631.
17 Y. Mir, P. Auroy and L. Auvray, Density profile of polyelectrolyte brushes, *Phys. Rev. Lett.*, 1995, **75**, 2863–2866.
18 M. Balastre, F. Li, P. Schorr, J. Yang, J. W. Mays and M. V. Tirrell, A Study of Polyelectrolyte Brushes Formed from Adsorption of Amphiphilic Diblock Copolymers Using the Surface Forces Apparatus, *Macromolecules*, 2002, **35**, 9480–9486.
19 X. Guo and M. Ballauff, Spherical polyelectrolyte brushes: Comparison between annealed and quenched brushes, *Phys. Rev. E*, 2001, **64**, 0514061–0514069.

20 G. Romet-Lemonne, J. Daillant, P. Guenoun, J. Yang and J. W. Mays, Thickness and Density Profiles of Polyelectrolyte Brushes: Dependence on Grafting Density and Salt Concentration, *Phys. Rev. Lett.*, 2004, **93**, 148301–148304.
21 H. Ahrens, S. Förster and C. A. Helm, Polyelectrolyte brushes grafted at the air/water interface, *Macromolecules*, 1997, **30**, 8447–8452.
22 N. Ayres, S. G. Boyes and W. J. Brittain, Stimuli-Responsive Polyelectrolyte Polymer Brushes Prepared via Atom-Transfer Radical Polymerization, *Langmuir*, 2007, **23**, 182–189.
23 Z. Xiong, B. Peng, X. Han, C. Peng, H. Liu and Y. Hu, Dual-stimuli responsive behaviors of diblock polyampholyte PDMAEMA-b-PAA in aqueous solution, *J. Colloid Interface Sci.*, 2011, **356**, 557–565.
24 K. Yu and Y. Han, Effect of block sequence and block length on the stimuli-responsive behavior of polyampholyte brushes: hydrogen bonding and electrostatic interaction as the driving force for surface rearrangement, *Soft Matter*, 2009, **5**, 759–768.
25 Y. K. Jhon, S. Arifuzzaman, A. E. Özçam, D. J. Kiserow and J. Genzer, Formation of Polyampholyte Brushes via Controlled Radical Polymerization and Their Assembly in Solution, *Langmuir*, 2012, **28**, 872–882.
26 A. B. Lowe and C. L. McCormick, Synthesis and Solution Properties of Zwitterionic Polymers †, *Chem. Rev.*, 2002, **102**, 4177–4190.
27 N. Ayres, C. D. Cyrus and W. J. Brittain, Stimuli-responsive surfaces using polyampholyte polymer brushes prepared via atom transfer radical polymerization, *Langmuir*, 2007, **23**, 3744–3749.
28 S. Sanjuan and Y. Tran, Synthesis of random polyampholyte brushes by atom transfer radical polymerization, *J. Polym. Sci. Part Polym. Chem.*, 2008, **46**, 4305–4319.
29 S. Sanjuan and Y. Tran, Stimuli-Responsive Interfaces Using Random Polyampholyte Brushes, *Macromolecules*, 2008, **41**, 8721–8728.
30 E. Ji, D. G. Whitten and K. S. Schanze, pH-Dependent Optical Properties of a Poly(phenylene ethynylene) Conjugated Polyampholyte, *Langmuir*, 2011, **27**, 1565–1568.
31 P. G. Higgs and J.-F. Joanny, Theory of polyampholyte solutions, *J. Chem. Phys.*, 1991, **94**, 1543–1554.
32 A. Akinchina, N. P. Shusharina and P. Linse, Diblock Polyampholytes Grafted onto Spherical Particles: Monte Carlo Simulation and Lattice Mean-Field Theory, *Langmuir*, 2004, **20**, 10351–10360.
33 N. P. Shusharina, E. B. Zhulina, A. V. Dobrynin and M. Rubinstein, Scaling Theory of Diblock Polyampholyte Solutions, *Macromolecules*, 2005, **38**, 8870–8881.
34 L.-J. Qu, X. Man, C. C. Han, D. Qiu and D. Yan, Responsive Behaviors of Diblock Polyampholyte Brushes within Self-Consistent Field Theory, *J. Phys. Chem. B*, 2012, **116**, 743–750.
35 V. Yamakov, A. Milchev, H. J. Limbach, B. Dünweg and R. Everaers, Conformations of random polyampholytes, *Phys. Rev. Lett.*, 2000, **85**, 4305–4308.
36 R. K. Das and R. V. Pappu, Conformations of intrinsically disordered proteins are influenced by linear sequence distributions of oppositely charged residues, *Proc. Natl. Acad. Sci.*, 2013, **110**, 13392–13397.
37 D. Srivastava and M. Muthukumar, Sequence dependence of conformations of polyampholytes, *Macromolecules*, 1996, **29**, 2324–2326.
38 J. N. Bright, M. J. Stevens, J. Hoh and T. B. Woolf, Characterizing the function of unstructured proteins: Simulations of charged polymers under confinement, *J. Chem. Phys.*, 2001, **115**, 4909–4918.
39 Q. Cao and H. You, Morphologies of spherical polyampholyte brushes: Effects of counterion valence and charged monomer sequence, *Polymer*, 2017, **113**, 233–246.

40 M. Baratlo and H. Fazli, Brushes of flexible, semiflexible, and rodlike diblock polyampholytes: Molecular dynamics simulation and scaling analysis, *Phys. Rev. E*, 2010, **81**, 011801–011807.
41 M. Baratlo and H. Fazli, Molecular dynamics simulation of semiflexible polyampholyte brushes--The effect of charged monomers sequence, *Eur. Phys. J. E*, 2009, **29**, 131–138.
42 T. E. Patten and K. Matyjaszewski, Atom Transfer Radical Polymerization and the Synthesis of Polymeric Materials, *Adv. Mater.*, 1998, **10**, 901–915.
43 T. Ando, M. Kato, M. Kamigaito and M. Sawamoto, Living Radical Polymerization of Methyl Methacrylate with Ruthenium Complex: Formation of Polymers with Controlled Molecular Weights and Very Narrow Distributions, *Macromolecules*, 1996, **29**, 1070–1072.
44 K. Matyjaszewski, T. E. Patten and J. Xia, Controlled/"living" radical polymerization. Kinetics of the homogeneous atom transfer radical polymerization of styrene, *J. Am. Chem. Soc.*, 1997, **119**, 674–680.
45 K. Matyjaszewski, H. Dong, W. Jakubowski, J. Pietrasik and A. Kusumo, Grafting from Surfaces for "Everyone": ARGET ATRP in the Presence of Air, *Langmuir*, 2007, **23**, 4528–4531.
46 W. Jakubowski and K. Matyjaszewski, Activators Regenerated by Electron Transfer for Atom-Transfer Radical Polymerization of (Meth)acrylates and Related Block Copolymers, *Angew. Chem. Int. Ed.*, 2006, **45**, 4482–4486.
47 K. Min, H. Gao and K. Matyjaszewski, Use of Ascorbic Acid as Reducing Agent for Synthesis of Well-Defined Polymers by ARGET ATRP, *Macromolecules*, 2007, **40**, 1789–1791.
48 J. Pietrasik, H. Dong and K. Matyjaszewski, Synthesis of High Molecular Weight Poly(styrene- *co* -acrylonitrile) Copolymers with Controlled Architecture, *Macromolecules*, 2006, **39**, 6384–6390.
49 H. Dong, W. Tang and K. Matyjaszewski, Well-Defined High-Molecular-Weight Polyacrylonitrile via Activators Regenerated by Electron Transfer ATRP, *Macromolecules*, 2007, **40**, 2974–2977.
50 L. Mueller, W. Jakubowski, W. Tang and K. Matyjaszewski, Successful Chain Extension of Polyacrylate and Polystyrene Macroinitiators with Methacrylates in an ARGET and ICAR ATRP, *Macromolecules*, 2007, **40**, 6464–6472.
51 J. Pietrasik, C. M. Hui, W. Chaladaj, H. Dong, J. Choi, J. Jurczak, M. R. Bockstaller and K. Matyjaszewski, Silica-Polymethacrylate Hybrid Particles Synthesized Using High-Pressure Atom Transfer Radical Polymerization, *Macromol. Rapid Commun.*, 2011, **32**, 295–301.
52 Y. Shen, H. Tang and S. Ding, Catalyst separation in atom transfer radical polymerization, *Prog. Polym. Sci.*, 2004, **29**, 1053–1078.
53 W. Lin, S. Nie, Q. Zhong, Y. Yang, C. Cai, J. Wang and L. Zhang, Amphiphilic miktoarm star copolymer (PCL)3-(PDEAEMA-b-PPEGMA)3 as pH-sensitive micelles in the delivery of anticancer drug, *J. Mater. Chem. B*, 2014, **2**, 4008–4020.
54 P. V. Mendonça, S. E. Averick, D. Konkolewicz, A. C. Serra, A. V. Popov, T. Guliashvili, K. Matyjaszewski and J. F. J. Coelho, Straightforward ARGET ATRP for the Synthesis of Primary Amine Polymethacrylate with Improved Chain-End Functionality under Mild Reaction Conditions, *Macromolecules*, 2014, **47**, 4615–4621.
55 H. Tang, M. Radosz and Y. Shen, CuBr2/N,N,N′,N′-Tetra[(2-pyridal)methyl]ethylenediamine/Tertiary Amine as a Highly Active and Versatile Catalyst for Atom-Transfer Radical Polymerization via Activator Generated by Electron Transfer, *Macromol. Rapid Commun.*, 2006, **27**, 1127–1131.
56 S. Tugulu, A. Arnold, I. Sielaff, K. Johnsson and H.-A. Klok, Protein-functionalized polymer brushes, *Biomacromolecules*, 2005, **6**, 1602–1607.
57 C. Deodhar, E. Soto-Cantu, D. Uhrig, P. Bonnesen, B. S. Lokitz, J. F. Ankner and S. M. Kilbey, Hydration in Weak Polyelectrolyte Brushes, *ACS Macro Lett.*, 2013, **2**, 398–402.

58 Y. Shen, S. Desseaux, B. Aden, B. S. Lokitz, S. M. Kilbey, Z. Li and H.-A. Klok, Shape-Persistent, Thermoresponsive Polypeptide Brushes Prepared by Vapor Deposition Surface-Initiated Ring-Opening Polymerization of α-Amino Acid *N* -Carboxyanhydrides, *Macromolecules*, 2015, **48**, 2399–2406.
59 S. B. Rahane, J. A. Floyd, A. T. Metters and S. M. Kilbey, Swelling Behavior of Multiresponsive Poly(methacrylic acid)-block--poly(N-isopropylacrylamide) Brushes Synthesized Using Surface-Initiated Photoiniferter-Mediated Photopolymerization, *Adv. Funct. Mater.*, 2008, **18**, 1232–1240.
60 J. P. Hinestrosa, J. Alonzo, J. W. Mays and S. M. Kilbey, Role of Surface Reorganization on Preferential Adsorption of Macromolecular Ensembles at the Solid/Fluid Interface, *Macromolecules*, 2009, **42**, 7913–7918.
61 J. Alonzo, J. P. Hinestrosa, J. W. Mays and S. M. Kilbey, Kinetics of Preferential Adsorption of Amphiphilic Star Block Copolymers that Tether by Their Corona Blocks at the Solid/Fluid Interface, *Macromolecules*, 2014, **47**, 4048–4055.
62 A. Y. Sankhe, S. M. Husson and S. M. Kilbey, Effect of Catalyst Deactivation on Polymerization of Electrolytes by Surface-Confined Atom Transfer Radical Polymerization in Aqueous Solutions, *Macromolecules*, 2006, **39**, 1376–1383.
63 K. A. Davis and K. Matyjaszewski, Atom Transfer Radical Polymerization of *tert* -Butyl Acrylate and Preparation of Block Copolymers, *Macromolecules*, 2000, **33**, 4039–4047.
64 B. Zhao and W. J. Brittain, Synthesis, Characterization, and Properties of Tethered Polystyrene- *b* -polyacrylate Brushes on Flat Silicate Substrates, *Macromolecules*, 2000, **33**, 8813–8820.
65 X. Kong, T. Kawai, J. Abe and T. Iyoda, Amphiphilic Polymer Brushes Grown from the Silicon Surface by Atom Transfer Radical Polymerization, *Macromolecules*, 2001, **34**, 1837–1844.
66 M. Ejaz, K. Ohno, Y. Tsujii and T. Fukuda, Controlled Grafting of a Well-Defined Glycopolymer on a Solid Surface by Surface-Initiated Atom Transfer Radical Polymerization, *Macromolecules*, 2000, **33**, 2870–2874.
67 H. Dong and K. Matyjaszewski, ARGET ATRP of 2-(Dimethylamino)ethyl Methacrylate as an Intrinsic Reducing Agent, *Macromolecules*, 2008, **41**, 6868–6870.
68 J. F. Weiss, G. Tollin and J. T. Yoke III, Reactions of triethylamine with copper halides. II. Internal oxidation-reduction of dichlorobis (triethylamine) copper (II), *Inorg. Chem.*, 1964, **3**, 1344–1348.
69 J. D. Willott, T. J. Murdoch, B. A. Humphreys, S. Edmondson, G. B. Webber and E. J. Wanless, Critical Salt Effects in the Swelling Behavior of a Weak Polybasic Brush, *Langmuir*, 2014, **30**, 1827–1836.
70 P. van de Wetering, E. E. Moret, N. M. E. Schuurmans-Nieuwenbroek, M. J. van Steenbergen and W. E. Hennink, Structure−Activity Relationships of Water-Soluble Cationic Methacrylate/Methacrylamide Polymers for Nonviral Gene Delivery, *Bioconjug. Chem.*, 1999, **10**, 589–597.
71 J. D. Willott, T. J. Murdoch, B. A. Humphreys, S. Edmondson, E. J. Wanless and G. B. Webber, Anion-Specific Effects on the Behavior of pH-Sensitive Polybasic Brushes, *Langmuir*, 2015, **31**, 3707–3717.
72 J. D. Willott, B. A. Humphreys, T. J. Murdoch, S. Edmondson, G. B. Webber and E. J. Wanless, Hydrophobic effects within the dynamic pH-response of polybasic tertiary amine methacrylate brushes, *Phys. Chem. Chem. Phys.*, 2015, **17**, 3880–3890.
73 Y. Shen, S. Desseaux, B. Aden, B. S. Lokitz, S. M. Kilbey, Z. Li and H.-A. Klok, Shape-Persistent, Thermoresponsive Polypeptide Brushes Prepared by Vapor Deposition Surface-Initiated Ring-Opening Polymerization of α-Amino Acid *N* -Carboxyanhydrides, *Macromolecules*, 2015, **48**, 2399–2406.

74 T. Wu, P. Gong, I. Szleifer, P. Vlček, V. Šubr and J. Genzer, Behavior of Surface-Anchored Poly(acrylic acid) Brushes with Grafting Density Gradients on Solid Substrates: 1. Experiment, *Macromolecules*, 2007, **40**, 8756–8764.
75 P. Gong, T. Wu, J. Genzer and I. Szleifer, Behavior of Surface-Anchored Poly(acrylic acid) Brushes with Grafting Density Gradients on Solid Substrates: 2. Theory, *Macromolecules*, 2007, **40**, 8765–8773.
76 R. Kumar, B. G. Sumpter and S. M. Kilbey, Charge regulation and local dielectric function in planar polyelectrolyte brushes, *J. Chem. Phys.*, 2012, **136**, 234901.
77 R. Dong, M. Lindau and C. K. Ober, Dissociation Behavior of Weak Polyelectrolyte Brushes on a Planar Surface, *Langmuir*, 2009, **25**, 4774–4779.
78 S. Ulrich, M. Seijo and S. Stoll, A Monte Carlo Study of Weak Polyampholytes: Stiffness and Primary Structure Influences on Titration Curves and Chain Conformations †, *J. Phys. Chem. B*, 2007, **111**, 8459–8467.
79 Turner Alfrey, Jr, Raymond M. Fous, H. Morawetz and H. Pinner, Amphoteric Polyelectrolytes. 11. Copolymers of Methacrylic Acid and Diethylaminoethyl Methacrylate, *J. Am. Chem. Soc.*, 1952, **74**, 438–441.
80 E. Stellwagen, J. D. Prantner and N. C. Stellwagen, Do zwitterions contribute to the ionic strength of a solution?, *Anal. Biochem.*, 2008, **373**, 407–409.
81 Y.-T. Liao, A. C. Manson, M. R. DeLyser, W. G. Noid and P. S. Cremer, Trimethylamine *N* -oxide stabilizes proteins via a distinct mechanism compared with betaine and glycine, *Proc. Natl. Acad. Sci.*, 2017, **114**, 2479–2484.
82 S. Jamal, A. Kumari, A. Singh, S. Goyal and A. Grover, Conformational Ensembles of α-Synuclein Derived Peptide with Different Osmolytes from Temperature Replica Exchange Sampling, *Front. Neurosci.*, 2017, **11**, 1–11.
83 R. Politi and D. Harries, Enthalpically driven peptide stabilization by protective osmolytes, *Chem. Commun.*, 2010, **46**, 6449.
84 S. Sukenik, L. Sapir and D. Harries, Balance of enthalpy and entropy in depletion forces, *Curr. Opin. Colloid Interface Sci.*, 2013, **18**, 495–501.
85 N. Srinivasan, M. Bhagawati, B. Ananthanarayanan and S. Kumar, Stimuli-sensitive intrinsically disordered protein brushes, *Nat. Commun.*, 2014, **5**, 5145.

**Table of Contents Graphic and Text**

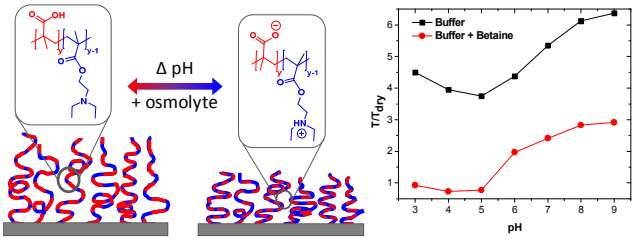


Local comonomer sequence of random polyampholyte brushes synthesized by ARGET ATRP facilitates ionization and promotes self-neutralization across a wide pH range, including in the presence of an added osmolyte.